Three-dimensional theory of the free-electron laser. I. Gain and evolution of optical modes

Avner Amir and Yuval Greenzweig
Quantum Institute and Department of Physics, University of California, Santa Barbara, California 93106
(Received 22 November 1985)

A three-dimensional free-electron-laser theory in the small-signal regime is presented. In the first part, we derive an energy theorem which relates the gain and the loss of an optical beam of arbitrary shape, driven by an electron beam of arbitrary profile. We show how this theorem can be applied for gain calculation and optimum resonator design. In the second part, we introduce a generalized description of a Gaussian optical beam. This includes four real parameters: the on-axis intensity and phase, the beam waist, and its radius of curvature. These quantities are made to evolve self-consistently and are governed by a set of ordinary differential equations which are readily integrated numerically. The solution of these equations provides an easy and intuitive means for the understanding of transverse effects induced by the interaction with the electron beam in a way which is considerably simpler than the more accurate large-scale simulation techniques.

INTRODUCTION

In the free-electron laser (FEL), a beam of relativistic electrons moves through a periodic magnetic field (undulator or wiggler) while interacting with an optical beam stored in a resonator.

The details of the start-up, amplification, and saturation processes of the FEL oscillator have been the subject of extensive research in the past few years[1] based on one-dimensional (1D) theories. The 1D model enabled one to discuss the topics of small-signal-gain spectrum,[2] efficiency enhancement schemes,[3] and pulse propagation.[4] The results obtained were generally in good agreement with the observations made in the first two machines that became operational.[5–7] Both were low-gain machines and employed short electron-beam pulses in which the longitudinal effects were dominant.

The need for a three-dimensional description has arised especially since the recent operation of a new machine[8] and the construction of another[9] which incorporate high-gain design. In such lasers the structure of the optical mode will be largely influenced by the transverse effects and may differ significantly from the well-known[10] empty-cavity modes.

In contrast to one-dimensional models where light is allowed to propagate in only one direction, one may anticipate some fundamentally new phenomena such as transverse multimode behavior,[11] focusing,[12,13] and trapping[13] of the optical mode as a result of the interaction with the gain medium, which have been observed in conventional lasers.

The term *focusing* is used whenever the interaction has the effect of a positive lens (i.e., the geometrical rays bend toward the axis). Beam *trapping* is understood as a situation where the optical mode propagates down the axis without large-scale diffraction and the optical power is kept confined in the transverse plane as a result of the interaction. (This term should not be confused with a similar term from 1D FEL theory which is related to the confinement of electron orbits in phase space.) In conventional lasers higher-order phenomena such as self-focusing and self-trapping have also been considered.[13] Self-action is understood when a nonlinear term of the interaction is included and its effect is pictured by means of a field-dependent index of refraction. This work will be concerned with linear theory only and we shall refer to focusing and trapping caused by the lowest-order, linear change in the index of refraction caused by the presence of the electron beam. This change may lead, among other possibilities, to the process of optical guiding similar to that which takes place inside an optical fiber.[14]

The standard linear methods of optics usually deal with a light beam whose initial transverse profile is known and calculate its propagation in free space.[15] The difficulty in treating the full FEL problem lies in incorporating the optical-beam–electron-beam interaction, which evolves along the axis into the picture. For strong fields, the interaction tends to be highly nonlinear and requires numerical computation even in the simpler one-dimensional model.

Previous works on this subject may be classified roughly in the following categories.

(a) Single-pass amplifier treatments.[16–19] In this configuration which was realized in gain measurement experiments, a semianalytical expression for the single-pass gain and phase modulation of the input mode was evaluated in the low-gain, small-signal regime. For discussion of the saturation phase of the FEL oscillator, certain assumptions concerning the electron dynamics had to be made, such as "freezing" its phase with respect to the light beam phase.

(b) Self-consistent multipass calculations. These include purely numerical Fox-Li[20]-type approaches[21–24] and mode expansion techniques.[25–29] In the former group, the wave front was propagated back and forth between the resonator mirrors employing numerical integration with a paraxial kernel. In the latter, the kernel was explicitly expressed in terms of free-propagation modes or its spatial Fourier components, resulting in simplification of the transverse integrals involved. In both cases the process

was iterated successively until a steady-state oscillator mode was reached. These treatments were inspired by similar calculations done in the context of conventional lasers.[30–32]

(c) Other, more recent works[33,34] have considered FEL optically guided modes by treating the interaction region as a dielectric channel. The index of refraction of this channel was computed analytically from the linearized FEL equation and compared to numerical results obtained by particle simulations. These studies were undertaken as a result of current interest in a high-gain device operating in a short-wavelength region for which good reflectors are not available.[9]

The object of the present article is to provide some simple and intuitive means for the understanding of the transverse mode evolution in the FEL interaction. This is in contrast to most of the works mentioned above which emphasized a more accurate approach and turned out to be computationally involved in many cases.

This paper consists of five sections. In Secs. I and II, we summarize the linear FEL theory based on the coupled Maxwell-Lorentz equations. In Sec. III we derive from it an energy theorem that relates the change in the optical power, the FEL gain, and the diffraction losses in the resonator in the linear regime. This theorem is valid in the low- and high-gain regime and can be applied provided one has an *a priori* knowledge of the mode structure. We demonstrate its use in calculating the gain in some simple cases.

In Sec. V, a general "Gaussian-like" form is assumed for the optical beam. The beam is then characterized by only four real parameters that are allowed to vary self-consistently along the interaction region. These quantities are the on-axis intensity and phase, the beam waist, and its radius of curvature. Our theory yields a set of coupled ordinary differential equations for these parameters. The equations are easily solved numerically and one obtains a good deal of information about the beam deformation near the axis for various regions of the gain and the detuning parameter.

I. THE PENDULUM AND THE PARABOLIC WAVE EQUATIONS

The FEL problem is normally described by an equation of motion for the electron beam derived from the Lorentz force equation coupled with a field equation derived from Maxwell's equations.[2] Consider an electron beam perfectly injected into a helical undulator of length L and period $\lambda_0=2\pi/k_0$, where the magnetic field is $\mathbf{B}=B_0(\cos(k_0z),\sin(k_0z,0))$. The electron will move in helical orbits with velocity $c\boldsymbol{\beta}=c(-\beta_t\cos(k_0z), -\beta_t\sin(k_0z),\beta_0)$, where $c\beta_t$ is the transverse velocity, $\beta_t=K/\gamma$ (for a linear undulator, replace K/γ by the rms velocity $K/\sqrt{2}\gamma$), where $K\equiv eB\lambda_0/2\pi mc^2$. $c\beta_0$ is the injection longitudinal velocity, e is the magnitude of the electron charge, m is the electron mass, c is the speed of light, and γ as usual, defined by $\gamma=(1-\beta_0^2)^{-1/2}$. Under the scalar approximation the optical field is taken to have a polarization similar to that of the spontaneous emission from electrons in the undulator. The field is described in terms of a carrier wave of frequency that is slowly modulated in amplitude $\mathbf{E}(\mathbf{r},t)$ and phase $\varphi(\mathbf{r},t)$. The vector potential is $\mathbf{A}=|\mathbf{E}|(\sin\psi,\cos\psi,0)/k$ where $\psi=kz-\omega t+\varphi(\mathbf{r},t)$, $\omega=kc$, and $\lambda=2\pi/k$ is the optical wavelength. When $\mathbf{A}(\mathbf{r},t)$ is inserted into Maxwell equations and an average is made over many wavelengths of the optical beam, it results in the inhomogeneous parabolic wave equation[27]

$$\left[-\frac{i}{4}\tilde{\nabla}^2+\frac{\partial}{\partial\tau}\right]a(\tilde{\mathbf{r}},\tilde{z},\tau)=-\langle je^{-i\zeta}\rangle_{\tilde{\mathbf{r}},\tilde{z}+s\tau,\tau}\,. \tag{1.1}$$

Here $\tilde{\mathbf{r}}=(\tilde{x},\tilde{y})=(x,y)(k/2L)^{1/2}$, t and z have been transformed to $\tau=ct/L$, $\tilde{z}=(z-ct)/\delta$ where δ is the electron pulse length (here we will assume long pulses so $\delta=L$). $\tilde{\nabla}^2=\partial^2/\partial\tilde{x}^2+\partial^2/\partial\tilde{y}^2$ accounts for the diffraction in the transverse plane. The transverse scaling distance $(2L/k)^{1/2}$ is a characteristic distance associated with the diffraction. The quantity $j(\mathbf{r},\tau)=8\pi^2Ne^2\beta_t^2L^2\rho(\mathbf{r},\tau)/\gamma mc^2$ is related to the current density of the beam. $a(\mathbf{r},\tau)=4\pi NeKLE(\mathbf{r},\tau)/\gamma^2mc^2$ is the normalized electric field. The lag of the electron beam with respect to the optical beam over one undulator length is given by the normalized slippage $s=(1-\beta_0)L/\delta$. We neglect the interaction between longitudinal modes (which is mostly important in short-pulse FEL's) and set $s=0$. $\langle\ \rangle$ is an average over electrons in one wavelength of light. The electron phase ζ is defined as $\zeta=(k+k_0)z-\omega t$. The current in the right-hand side of (1.1) consists of many electrons obeying Lorentz's force equation $\dot{\gamma}=c\boldsymbol{\beta}\cdot(\partial\mathbf{A}/\partial t)mc^2$. Using the definitions of $\boldsymbol{\beta}$, ζ, $\mathbf{A}$, and a, this equation takes on the form of the so-called "pendulum equation"

$$\frac{d^2\zeta}{d\tau^2}=\tfrac{1}{2}(ae^{i\zeta}+\text{c.c.})\,. \tag{1.2}$$

Equations (1.1) and (1.2) without the diffraction operator have been used extensively before in 1D calculations.[1] Our purpose is to develop a similar theory that will emphasize the spatial mode characteristics of the problem.

II. LINEAR FEL THEORY

Equations (1.1) and (1.2) are quite general and are capable of describing the evolution of the optical and electron beam for a wide range of the field parameter a. For moderate to strong fields the nonlinear effects imbedded in (1.2) dominate the problem and one must resort to numerical methods.

Some analytical progress is possible if one assumes weak fields. To first order in small quantities we may write the electron phase as

$$\zeta=\zeta_0+\nu_0\tau+\delta\zeta\,, \tag{2.1}$$

where $\delta\zeta$ is of order a, so the electron phase is nearly linear in τ. This allows linearization of both Eqs. (1.1) and (1.2) by expanding and retaining terms of order a. Subsequent integration of Eq. (1.2) yields

$$\delta\zeta\approx\tfrac{1}{2}\int_{-1/2}^{\tau}\int_{-1/2}^{\tau'}(ae^{i\nu_0\tau''+i\zeta_0}+\text{c.c.})d\tau''\,d\tau'\,. \tag{2.2}$$

Note that the center of the wiggler is taken at the point

$\tau=0$. Upon substituting $\delta\zeta$ into the linearized source term of Eq. (1.1) and averaging over a uniform initial phase distribution of monoenergetic electrons in phase space we arrive at the following linear equation for the field:

$$\left[-\frac{i}{4}\tilde{\nabla}^2+\frac{\partial}{\partial\tau}\right]a(\tilde{\mathbf{r}},\tau) = \tfrac{1}{2}ij(\tilde{\mathbf{r}},\tau)\int_{-1/2}^{\tau}\int_{-1/2}^{\tau'}a(\tilde{\mathbf{r}},\tau'')e^{i\nu_0(\tau''-\tau)}d\tau'\,d\tau'' . \tag{2.3}$$

This equation describes the 3D evolution of the slowly varying part of the optical field in interaction with an electron beam of a transverse structure, while consistently accounting for the resulting electron motion in phase space.

III. ENERGY FLOW IN THE FEL 3D GAIN FORMULA

Setting $a=|a|e^{i\varphi}$ in (2.3) and separating the real and imaginary parts of the equation, multiplying the former by a^* and dividing the latter by a yields (from here on we omit the tildes over the transverse coordinates):

$$\tfrac{1}{2}|a|\nabla\varphi\cdot\nabla|a|+\tfrac{1}{4}|a|^2\nabla^2\varphi+|a|\frac{\partial|a|}{\partial\tau} = \mathrm{Re}\tfrac{1}{2}ij(\mathbf{r},\tau) \times\int_{-1/2}^{\tau}d\tau'(\tau-\tau')a(\mathbf{r},\tau')a^*(\mathbf{r},\tau)e^{-i\nu_0(\tau-\tau')} , \tag{3.1a}$$

$$\tfrac{1}{4}|\nabla\varphi|^2+\frac{\partial\varphi}{\partial\tau} = \frac{1}{4}\frac{\nabla^2|a|}{|a|} +\mathrm{Im}\tfrac{1}{2}ij(\mathbf{r},\tau)\int_{-1/2}^{\tau}d\tau'(\tau-\tau')\frac{a(\mathbf{r},\tau')}{a(\mathbf{r},\tau)}e^{-i\nu_0(\tau-\tau')} , \tag{3.1b}$$

where in the conversion to a single integral we used a method described in Appendix A.

Integrating Eq. (3.1a) over an arbitrary region in the transverse plane we obtain

$$\frac{\partial}{\partial\tau}\int|a|^2d^2\tau=\mathrm{Re}\,i\int d^2r\,j(\mathbf{r},\tau)\int_{-1/2}^{\tau}d\tau'(\tau-\tau')a^*(\mathbf{r},\tau)a(\mathbf{r},\tau')e^{-i\nu_0(\tau-\tau')}-\tfrac{1}{2}\int\nabla\cdot(|a|^2\nabla\varphi)d^2\tau . \tag{3.2}$$

Equation (3.2) is an energy statement which says that the change in the optical power experienced by the beam while propagating through a region of arbitrary cross section equals the gain (the first term on the right) minus the amount of power lost because of diffraction or increased due to focusing (the second term on the right).

The last integral on the right-hand side may be converted to a surface integral which will simplify its evaluation in most cases. In the limit of a large Fresnel number, this term will vanish when a is a cavity mode.

Integrating over the time spent in one pass along the wiggler, and using the methods of Appendix A results in the following expression for the power increment $\delta P_{\mathrm{pass}}\equiv\int d^2r[|a(\frac{1}{2})|^2-|a(-\frac{1}{2})|^2]$:

$$\delta P_{\mathrm{pass}}=-\frac{1}{2}\frac{\partial}{\partial\nu_0}\int d^2r\,j(\mathbf{r})\left|\int_{-1/2}^{1/2}d\tau e^{i\nu_0\tau}a(\mathbf{r},\tau)\right|^2 -\tfrac{1}{2}\int_{-1/2}^{1/2}d\tau\int\nabla\cdot(|a|^2\nabla\varphi)d^2r ,$$

where the transverse integration is carried over the resonator cross section. We have dropped the τ dependence in the current profile assuming it is constant along the interaction region and thus excluded transverse effects such as finite beam emittance and betatron oscillations. The first term on the right-hand side when divided by the input power is identified as the gain per pass:

$$G=-\frac{1}{2P_{\mathrm{in}}}\frac{\partial}{\partial\nu_0}\int d^2r\,j(\mathbf{r})\left|\int_{-1/2}^{1/2}d\tau e^{i\nu_0\tau}a(\mathbf{r},\tau)\right|^2 . \tag{3.3}$$

In order to evaluate it without explicitly solving Eq. (2.3) some assumptions concerning the mode $a(\mathbf{r},\tau)$ are necessary. It is common practice to choose one of the passive cavity modes (usually the fundamental). This is intuitively justified in the case of low gain. In the high-gain case, Eq. (3.3) still holds but may prove to be useless in the absence of information about the prevailing mode. In a high-gain amplifier the injected mode will certainly undergo considerable reshaping as a result of the interaction. The latter case will be dealt with in Sec. V. We also note that since the dependence of the mode on ν_0 has not become explicit (the derivative is a partial derivative and acts only on the exponent) one cannot use this equation, in the high-gain case, to calculate effects of beam energy dispersion as was done in 1D treatments.

Let us further remark here that Eq. (3.3) with a being a cavity mode (a member of a complete set of eigenmodes) may be considered an extension of a familiar expression relating the spontaneous and stimulated emission in 1D theories, known as Madey's theorem.[35] An expansion of the spontaneous emission in terms of resonator modes has been given in Ref. 36, where the expansion coefficients have a similar form to the quantity to be differentiated in Eq. (3.3). Unlike the 1D theory, due to the extra degrees of freedom, the 3D mode appearing in (3.3) will be characterized by a frequency (or a longitudinal index) and two transverse indices. Expression (3.3) can be used for optimizing the laser gain by choosing the appropriate values for the parameters of a given optical mode, as will be shown in the next section. It is interesting to point out that in contrast to many conventional lasers, most FEL's tend to have gain media that are much narrower than the

optical beams. It is therefore conceivable (and indeed shown in Sec. IV) that a higher gain could be achieved were the laser mode made of a combination of passive cavity modes. Unfortunately, the oscillation frequencies of the cavity modes of different transverse indices are different in general which implies also different detuning parameters with respect to the electron beam. This situation may be avoided in confocal resonators which have degenerate mode spectra. These resonators are, however, on the edge of the geometrical stability region[10] and may not be suitable for practical design. Another interesting possibility along the same lines is mentioned in Ref. 29.

IV. THE GAIN IN SOME SIMPLE CASES

Let us now turn to some simple examples where an explicit expression for the single-pass gain may be written. The empty cavity modes are given in any standard text[10] by solving Eq. (2.3) with $j=0$. The fundamental mode, having an azimuthal symmetry, of the so-called Gaussian-Laguerre beams is given by

$$g_0(\mathbf{r},\tau)=\frac{a_0}{1+iq\tau}e^{-qr^2/(1+iq\tau)}. \tag{4.1}$$

We are using somewhat nonconventional notations which tend to produce short expressions. Following Ref. 18 we have defined $q=L/z_0$ where $z_0=\pi w_0^2/\lambda$ (known as the Rayleigh length) and w_0 is the beam waist. a_0 may be determined from the input power since $P_{\text{in}}=a_0^2\pi/2q$.

Consider first a cylindrical beam distributed at $r=r_0$ (in the special case $r_0=0$ we have a "filamentary" beam located on axis). Its current density is given by $j(\mathbf{r})=i_0\delta^2(r-r_0)$. Substitution in (3.3) gives

$$G=-\frac{qi_0}{\pi}\frac{\partial}{\partial\nu_0}\left|\int_{-1/2}^{1/2}d\tau\frac{e^{-qr_0^2/(1+iq\tau)+i\nu_0\tau}}{1+iq\tau}\right|^2, \tag{4.2}$$

where $i_0\equiv 8\pi^2Ne^2\beta_t^2L^2I(k/2L)/\gamma mc^3$, I being the total current in the beam. Equation (4.2) in a different form has appeared before,[18] where it was derived under different considerations that did not yield the proportionality constant in front.

A plot of the gain formula (4.2) for an on-axis ($r_0=0$) electron beam is given in Fig. 1 (the numerical computation is facilitated using a method described at the end of Appendix A). Different values of q mean different angular spreads of the photons forming the beam which results in an effective shift of the peak gain. From (4.2) we also note that at small values of q the gain is very nearly proportional to q (inversely proportional to the mode area). As q grows, the beam consists of photons diverging at larger angles which implies greater detuning for an electron moving along the axis. Eventually most of them contribute only to the tails of the 1D gain spectrum so that their total gain decreases. These considerations predict a maximum that is evident in Fig. 2, near $q=4$. The "finite angular acceptance" of the gain is the main mechanism by which the typically narrow FEL gain medium can select a transverse mode. When designing an actual resonator it is of course necessary to consider also the losses (diffractive or other) that will generally vary with q.

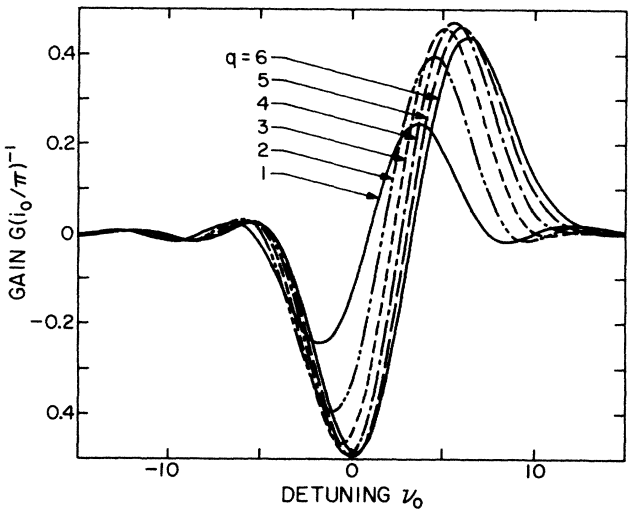

FIG. 1. Gain as a function of the detuning parameter ν_0 at different values of diffraction parameter q. Note the shift and the decrease in height of the peaks as q gets larger. This is due to the fact that the highly diffracted modes consist of many photons diverging at large angles with respect to the electron beam. In terms of the 1D model, such photons will have large detuning parameters and therefore lie at the tails of the gain curve. A combination of highly diverging photons also suffers an overall large phase shift with respect to axial photons for the same reason.

In the limit $q\to 0$ the integral in Eq. (4.2) can be calculated [explicit expressions in conventional (mks) units for

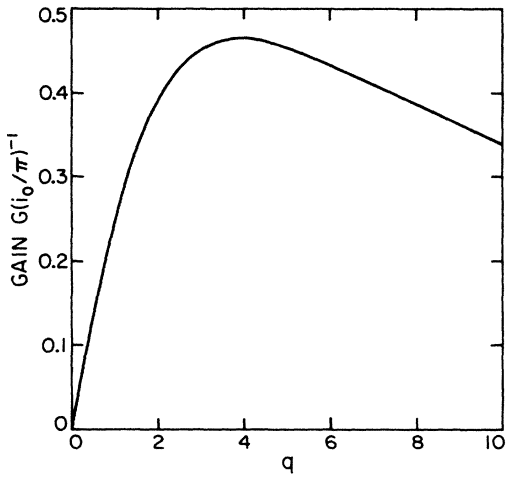

FIG. 2. Maxima of the curves in Fig. 1 as a function of q. At large q the beam diffracts and gain is reduced as discussed above. At small values, the on-axis field of the normalized mode decreases inversely proportional to the mode area, because of the larger spread of the energy and so that the gain also decreases as seen on the left part of the curve. The curve was obtained by first maximizing the gain over all values of ν_0 in Eq. (4.2).

the helically undulating beam interacting with an open resonator mode as well as linearly polarized beam interacting with a waveguide mode may be found in Ref. 37]. We find (taking $r_0=0$ for simplicity) that except for the phase shift, Eq. (4.2) agrees completely with the earlier 1D results that were corrected phenomenologically by a "filling factor,"[2] provided the optical mode area is taken as $\pi w_0^2/2$. Our theory has yielded this factor in a natural way.

As r_0 grows (Fig. 3) the gain magnitude shrinks due to the exponential falloff of the field. It is interesting to note that no significant phase shift is observed unless the gain is negligibly small.

A slightly more realistic electron-beam profile would be $j(\mathbf{r})=(i_0 q_e/\pi)e^{-q_e r^2}$, where q_e^{-1} is the characteristic beam area in our units (for actual dimensions, multiply by $2L/k$). With this current profile and the Gaussian beam in (4.1), the gain in Eq. (3.3) becomes, after performing the transverse integrals:

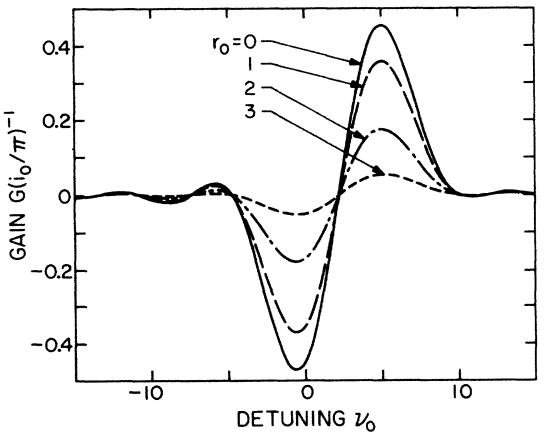

FIG. 3. Gain curves for cylindrical beams of various radii r_0. There is very little phase shift introduced unless the radius is so large that the gain is negligibly small. The diffraction parameter is $q=3$. Actual radius is normalized by $\sqrt{2L/k}$.

$$G=-\frac{2qi_0}{\pi}\mathrm{Re}\frac{\partial}{\partial\nu_0}\int_{-1/2}^{1/2}d\tau\int_{-1/2}^{\tau}d\tau'\frac{e^{-i\nu_0(\tau-\tau')}}{(1+iq\tau')(1-iq\tau)}\left[1+\frac{q}{q_e}\left[\frac{1}{1+iq\tau'}+\frac{1}{1-iq\tau}\right]\right]^{-1}. \tag{4.3}$$

Figures 4 and 5 are analogous to Figs. 1 and 2, respectively. In Fig. 4 we note that varying the beam area over 5 orders of magnitude does not yield any significant phase shifts. In light of Fig. 3 it is clear that electrons that are very far from the axis, which experience considerable phase shifts, have produced negligible contribution to the gain. For very wide electron beams (very small values of q_e) the gain curve will eventually shift but then the peak gain is already very small. For values $q_e \geq 10$ the gain curve is practically that of a filamentary beam (as in Fig. 1). We must keep in mind, however, that in the actual electron beam, finite beam emittance, and the wiggler field inhomogeneities will alter electron trajectories and consequently lower the gain seen in these curves. Electrons moving at an angle with respect to the axis will tend to drive photons which correspond to detuning parameters off the peak of Fig. 1 making it broader and the peak gain smaller.

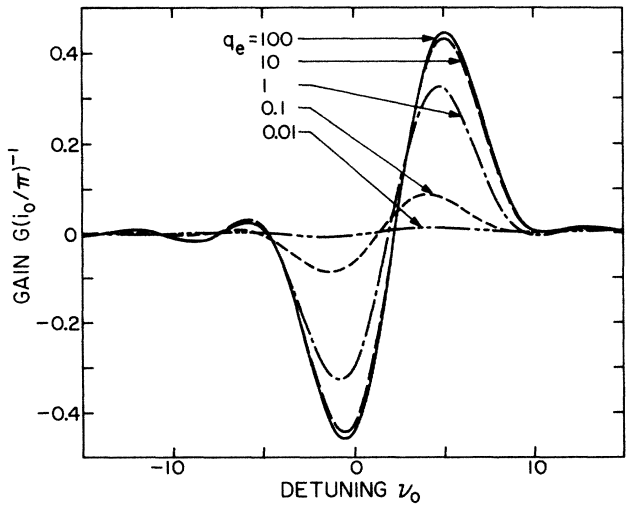

FIG. 4. Gain curves of Gaussian electron beams of different areas, computed from Eq. (4.3). Contribution of outer electrons, which experience substantial phase changes of the optical beam, to the gain, is very small (in accordance with Fig. 3). As a result the wider electron beams that sample large phase shifts tend to move the peak gain but the overall gain is diminished. Beam area in actual units is $q_e^{-1}(2L/k)$.

As a final example, let us consider a field composed of the first two azimuthally symmetric Laguerre-Gaussian modes which are different from zero at the center. The combination is given by

$$a=a_0\frac{1}{(1+|\alpha|^2)^{1/2}}(g_0+\alpha g_1), \tag{4.4}$$

where

$$g_0=e^{-qr^2/(1+iq\tau)}/(1+iq\tau),$$

$$g_1=g_0[1-2qr^2/(1+q^2\tau^2)](1-iq\tau)/(1+iq\tau).$$

Here α is a constant (complex in general) which describes the mode mixing and $(1+|\alpha|^2)^{1/2}$ is the normalization constant. As previously mentioned, these modes can be excited in a general resonator at different frequencies which will induce a relative detuning $\Delta\nu_0$ between the two. This shift can be taken into account by replacing the constant α by $\alpha e^{i\Delta\nu_0\tau}$ in the gain expression following. However, since the present theory was not constructed to account for the full multimode picture of the FEL oscillator, it will be inconsistent to introduce such an effect here. We may, however, treat the somewhat nonpractical case of a confocal resonator where transverse modes are frequency degenerate in order to get an idea about the gain

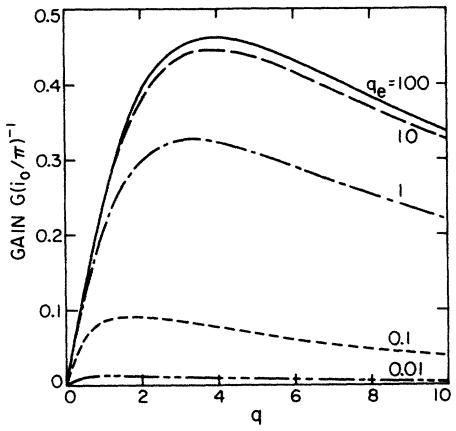

FIG. 5. Maxima of each of the curves in Fig. 4 as a function of q. For $q \geq 10$ the curve is practically equivalent to Fig. 2. Note the small shift of the maxima for very wide beams.

increase when the system is allowed "to choose" its desired combination of cavity modes. Inserting (4.4) into (3.3) with a filamentary beam at $r_0=0$, we obtain

$$G=-\frac{2qi_0}{\pi}\frac{1}{1+|\alpha|^2}\times\frac{\partial}{\partial\nu_0}\left|\int d\tau e^{i\nu_0\tau}\frac{1}{1+iq\tau}\left[1-\alpha\frac{1-iq\tau}{1+iq\tau}\right]\right|^2 . \tag{4.5}$$

In Fig. 6 we have plotted Eq. (4.5) at several real values of the coefficient α. In a confocal resonator, the value $q=2$ which maximizes the gain over all combinations should be selected. In a nonconfocal resonator designed for a single-mode laser, such a value should be avoided since it represents an inclination of the system to generate a large fraction of the higher-order mode by the gain

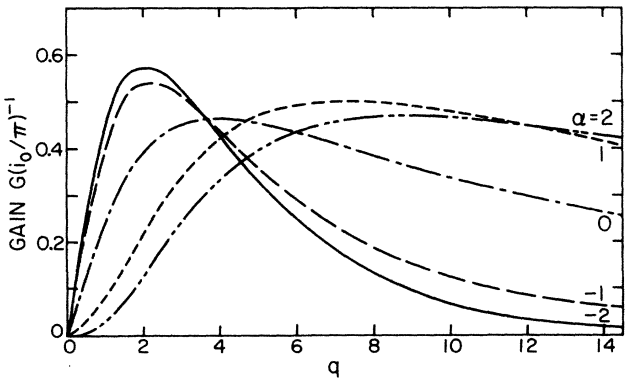

FIG. 6. Maximum gain curves for different combinations of the fundamental and the second higher-order azimuthally symmetric Gaussian-Laguerre modes [Eq. (4.5)] (indices 0 and 2). Maximum gain for the combination is obtained at a region around $q=4$ and gives about 20% more gain than the fundamental mode ($\alpha=0$) whose maximum lies near $q=2$.

medium. We note that choosing $q=4$ will ensure both a domination of the fundamental mode and optimum gain in that mode. A more accurate approach requires consideration of complex values of α as well as the inclusion of higher-order modes.

V. EVOLUTION OF THE SELF-CONSISTENT BEAM PARAMETERS

In this section we introduce a generalized form for the Gaussian beam in (4.1). Using this form we can solve Eq. (2.3) near the axis and describe the optical beam evolution through the interaction region in a fully self-consistent manner.

We begin by writing the field in the form $a=e^{\psi(\mathbf{r},\tau)}$ we shall confine our attention to a small region around the axis and to azimuthally symmetric fields, we expand ψ as follows: $\psi(\mathbf{r},\tau)\approx\psi_0(\tau)+r^2\psi_1(\tau)+\cdots$. This is analogous to the aberration expansion familiar from classical optics.[15] In terms of real functions we write

$$a=P_1(\tau)e^{iP_2(\tau)+[Q_1(\tau)+iQ_2(\tau)]r^2}+\cdots . \tag{5.1}$$

P_1,P_2,Q_1,Q_2 are real and may be interpreted (in a local sense) as the beam on-axis intensity and phase, inverse "beam waist," and inverse radius of curvature, respectively.

Neglecting orders higher than the quadratic will be referred to as "the near-axis expansion." This expansion will be valid for the case of relatively wide electron beams where boundary effects can be neglected. The introduction of narrow electron beams will necessitate the inclusion of higher-order transverse modes that will not be carried out here. If we keep, however, our discussion within this rather limited context we will be able to follow the evolution of the optical beam—an object that in the more general case requires extensive numerical computations. Important insight will be gained by looking at the lowest-order transverse corrections to the familiar one-dimensional theory.

Retaining only the lowest power of r^2 one may solve exactly[10] the homogeneous version of Eq. (1.1) to find the fundamental cavity mode having an azimuthal symmetry (4.1). For (4.1) one can write explicitly the beam parameters

$$P_1=a_0\frac{1}{(1+q^2\tau^2)^{1/2}},\quad Q_1=-\frac{q}{1+q^2\tau^2},\qquad P_2=-\tan^{-1}(q\tau),\quad Q_2=\frac{q^2\tau}{1+q^2\tau^2} . \tag{5.2}$$

Equation (5.1) is not inserted into (2.3); carrying out the derivatives and dividing both sides by $a(\tau)$ we obtain

$$\left[-iQ+\frac{P'}{P}\right]+(-iQ^2+Q')r^2+\cdots = \tfrac{1}{2}ij(\mathbf{r})\int_{-1/2}^{\tau}d\tau'(\tau-\tau')\frac{P(\tau')}{P(\tau)}\times e^{i\nu_0(\tau'-\tau)+[Q(\tau')-Q(\tau)]r^2+\cdots} , \tag{5.3}$$

where the notations $Q=Q_1+iQ_2$, $P=P_1e^{iP_2}$ have been used. In a similar fashion we expand the gain profile, assuming a parabolic form near the axis $j(\mathbf{r})=j_0(1-q_e r^2)$. Expanding the r-dependent part of the exponent and collecting similar powers of r^2 we arrive at the following set of complex equations:

$$-iQ+\frac{P'}{P}=\tfrac{1}{2}ij_0\int_{-1/2}^{\tau}d\tau'(\tau-\tau')\frac{P(\tau')}{P(\tau)}e^{i\nu_0(\tau'-\tau)}, \tag{5.4a}$$

$$-iQ^2+Q'=\tfrac{1}{2}ij_0\int_{-1/2}^{\tau}d\tau'(\tau-\tau')\frac{P(\tau')}{P(\tau)}\times\{-q_e+[Q(\tau')-Q(\tau)]\}e^{i\nu_0(\tau'-\tau)}. \tag{5.4b}$$

In the derivation of Eq. (5.4) we have relied upon the assumption that there exists a region near the axis where the field evolves locally, neglecting contributions from the outer region. The expansion that led to (5.4b) will be justified provided the quadratic terms in the exponent of (5.3) are kept small. This gives a measure for the size of the region of validity in the transverse plane

$$r^2\ll\frac{\pi}{\max\limits_{-1/2\le\tau\le 1/2}|\Delta Q|}, \tag{5.5}$$

where $\max|\Delta Q|$ is the maximum amplitude of the variation of Q over the specified interval [that is, the maximum value that the quantity $|Q(\tau_1)-Q(\tau_2)|$ may achieve when τ_1,τ_2 lie in the interval]. In a geometrical-optics picture, the region of validity is wide if light rays would not deflect much away from the axis (either as a result of the natural diffraction or the interaction with the electron beam).

It is clear from (5.5) that as ΔQ decreases the size of the region of validity increases and if there are no variations at all it is easily seen that Eqs. (5.3) and (5.4) become exact [i.e., no higher-order terms are needed and $Q(\tau')=Q(\tau)$]. Thus, from the set of the general solutions of (2.3) (with a parabolic current profile), those whose nature is most closely given by (5.3) may be described as the nearly trapped modes. The subject of trapping will be further investigated in a subsequent article.[38]

The various terms in Eq. (5.4) may be interpreted as follows. In the absence of the source term (proportional to j_0) one gets the free propagating mode solutions given in (5.2). When the right-hand-side terms are added, the first equation describes the change of field on axis. The interaction term in this equation is similar to that of 1D theories, with the exception of the term $-iQ$ on the left, which takes into account the effects of diffraction spread and focusing as felt on-axis (e.g., in a focused beam, the negative imaginary part of Q will cause an increase in P_1). The second equation describes the off-axis evolution of the beam. The term proportional to q_e comes from the transverse gradient of the electron beam. Its contribution may be discussed in the familiar terms of propagation in a medium with a quadratic index of refraction.[10,13,39] We note here that this index of refraction may include both a refractive and a dissipative or gain component. We will use the term "localization" to describe an amplification of the power near the axis without significant phase fronts distortion. Thus, the refractive and the gain part may lead to focusing and localization, respectively. The other part of the integral [containing $Q(\tau')-Q(\tau)$] is unique to our problem. It is related to the dynamics of Q in the same way as the right-hand side of (5.4a) drives P, and contains the first-order correction to the differential gain term $e^{i\nu_0(\tau'-\tau)}P(\tau')/P(\tau)$ for being evaluated off-axis. The field variations in the transverse plane lead to different electron-beam dynamics and different amounts of gain across this plane. Even if the electron beam was transversely homogeneous ($q_e=0$), that term alone may cause deformations in the beam curvature and waist.

As described in detail in Appendix B, Eqs. (5.4a) and (5.4b) may be easily transformed into a set of nonlinear, ordinary differential equations which is conveniently solved on a computer. For a single-pass problem, one may start with the initial values for a free mode (5.2) at the beginning of the wiggler ($\tau=-\frac{1}{2}$), and evaluate the propagation according to (5.4) until $\tau=\frac{1}{2}$. [If integration over the complete round trip is desired, the effect of the mirrors may be introduced by discontinuously changing Q_2 at the mirror position then set j_0 in (5.3) to zero and propagate it analytically to the other mirror where another phase transformation is needed to complete the cycle.]

In Figs. 7–10 [curve (a)] we plotted the homogeneous solution to (5.4). These are the free mode parameters as given by (5.2). We note that the beam waist decreases toward the middle and achieves a minimum at $\tau=0$. The phase fronts are flat at the center, reach a maximum curvature at the Rayleigh length $\tau=q^{-1}$, and flatten out as we move away from the center.

Let us now consider what happens when the FEL interaction is turned on. The numerical solution to Eqs. (5.4) is illustrated Figs. 7–10 [curves (b) and (c)] in two cases: (1) $q_e>q$, an electron beam having a sharper gradient then the optical mode [note that the value of q refers only to the initial condition and describes the beam everywhere in the transverse plane while $Q(\tau)$ for $\tau>0$ is only local in character] and (2) $q_e\approx 0$, an electron beam with zero gradient (which we may safely assume being much wider than the optical mode without violating our previous assumptions). The initial conditions are taken to be those of the free mode starting at a mirror with the correct radius of curvature to produce the given q according to (5.2).

Case (1) is illustrated in Figs. 7–10 [curve (b)]. The parameters chosen where $j_0=7$, $q=2$, $q_e=5$, and $\nu_0=0$. As is well known from the 1D theory, this value of ν_0 produces large phase shifts. Indeed, when comparing the curves (a) and (b) on Fig. 8, we observe the difference with respect to the free mode. The phase remains approximately constant over the last quarter of the trip. This indicates that the natural defocusing of the Gaussian beam has been prevented. Some extra focusing has also taken place. Note that the curve (b) of Fig. 8 is approximately constant at the last quarter of the trip and even curls upward slightly. It becomes even more obvious in curve (b)

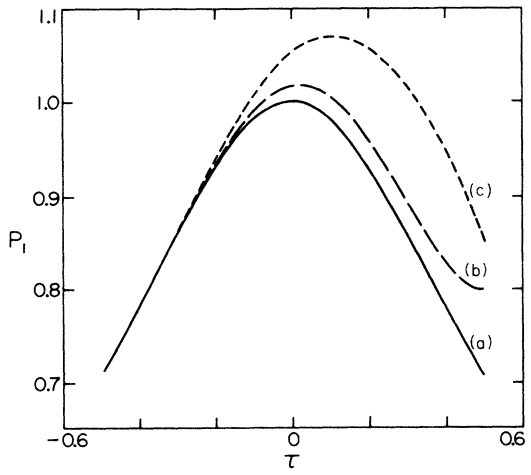

FIG. 7. Evolution of the parameter P_1. Figures 7–10 describe the evolution of the optical beam parameters P_1, P_2, Q_1, Q_2 as a function of τ [see Eq. (5.1) for definition] given by the numerical solution of Eqs. (5.4a) and (5.4b). Center of the wiggler ($\tau=0$) was taken to coincide with the minimum beam waist. In this example $q=2$. (a) Free mode. Beam is normalized so that $P_1=1$ at the center. Note that the maximum of Q_2 is obtained at the Rayleigh length ($=q^{-1}$). (b) Evolution under the interaction with a quadratic profile electron beam. Here $q_e=5$, $j_0=7$, $\nu_0=0$. Note that the on-axis intensity at $\tau=\frac{1}{2}$ is larger by about 10% than the initial value. This is due to significant phase distortion that has taken place as can be seen clearly in Figs. 8 and 10. (c) Evolution of the beam parameters under the interaction with an electron-beam profile much wider than the optical mode ($q_e=0$, $j_0=7$, $\nu_0=7$). Beam energy has concentrated near the axis ($|Q_1|$ has increased by about 0.5 overall) and the on-axis intensity grew by about 10% with not much distortion of the phases. This is evidence of near-axis power localization (see text) induced by the transversely inhomogeneous evolution of the gain medium.

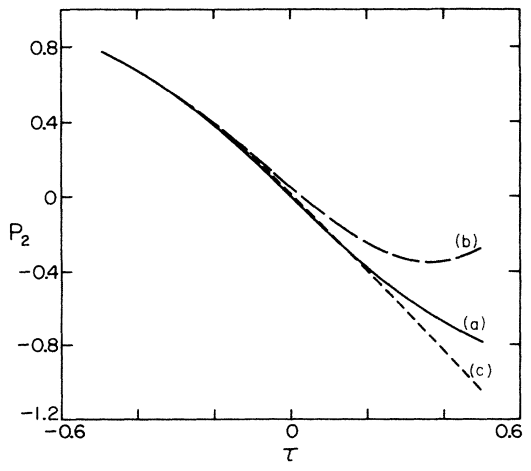

FIG. 8. Evolution of P_2. (Same case as Fig. 7.)

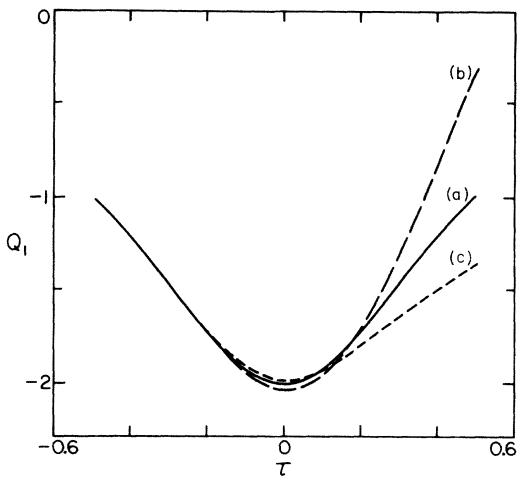

FIG. 9. Evolution of Q_1. (Same case as Fig. 7.)

of Fig. 10 where the negative part of Q_2 is apparent in that region. This focusing also results in more power on axis as seen when the curves (a) and (b) of Fig. 7 are compared at the end of the trip.

In this case then, the electron beam has acted as a converging lens, producing phase shifts that vary with the electron-beam profile. For other values of ν_0 the transverse gradient of the electron beam can produce localization when the real part of the gain becomes dominant.

Case (2) is illustrated in Figs. 7–10 [curve (c)]. The parameters taken were $j_0=7$, $q=3$, $q_e=0$, and $\nu_0=7$. This value of ν_0 was chosen since in its neighborhood the phase shifts are minimal. This is clear from curve (c) of Fig. 8 and curve (c) of Fig. 10. On the other hand, there is a larger on-axis gain seen on curve (c) of Fig. 7. The large gain causes the beam to grow considerably near the axis which induces even further growth. The growth has won over the natural decrease due to diffraction as shown on curve (c) of Fig. 9 where a net increase in the absolute value of Q_1 is evident at the end of the trip. This field-

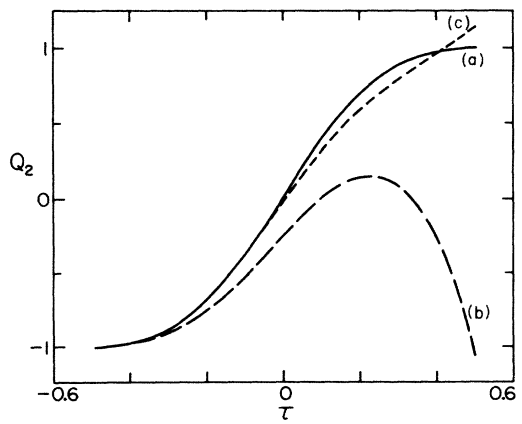

FIG. 10. Evolution of Q_2. (Same case as Fig. 7.)

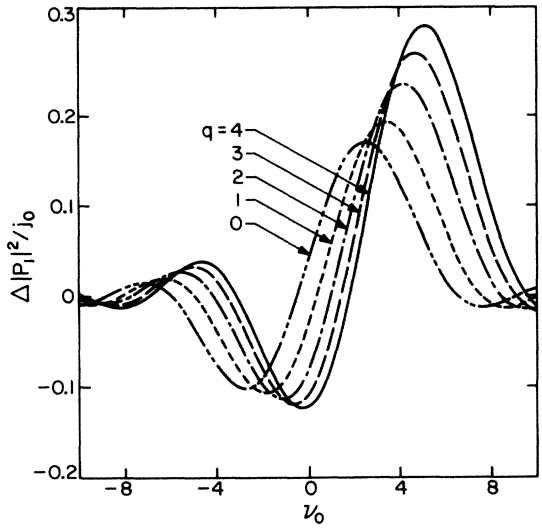

FIG. 11. Changes in P_1 as a function of the detuning ν_0 for different values of the diffraction parameter q. Figures 11—14 describe the changes in the optical-beam parameters (compare to a free mode at the end of the wiggler) as a function of ν_0 for a very wide electron beam ($q_e=0$, $j_0=7$) for various values of q. Electron beam has a homogeneous profile. Choice of q sets different initial conditions in each case. Note that the maxima of the localization and focusing occur at alternating points. Near $\nu_0=0$ strong defocusing and delocalization occur.

localization mechanism for wide electron beams is made possible by the nonlocal (in τ) nature of the FEL gain process as expressed by the second term on the right-hand side of Eq. (5.4b). The electron-beam dynamics evolves differently at different points in the transverse plane because of the transverse structure of the field. This results in inhomogeneous evolution of the gain across this plane. We note that the phase-fronts curvature has returned to its original value [Fig. 10(b)] with no significant net

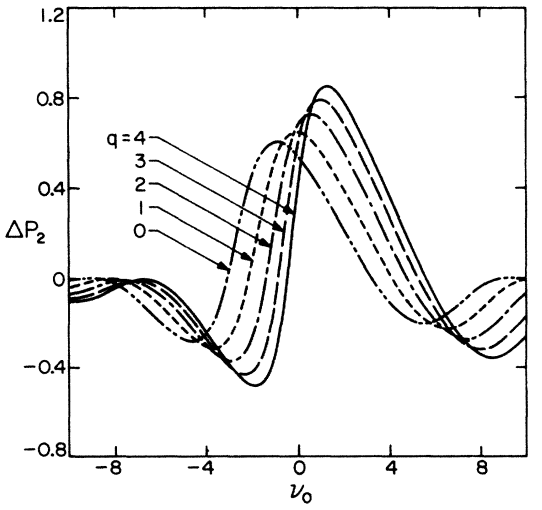

FIG. 12. Changes in P_2 as a function of ν_0. (Same case as Fig. 11.)

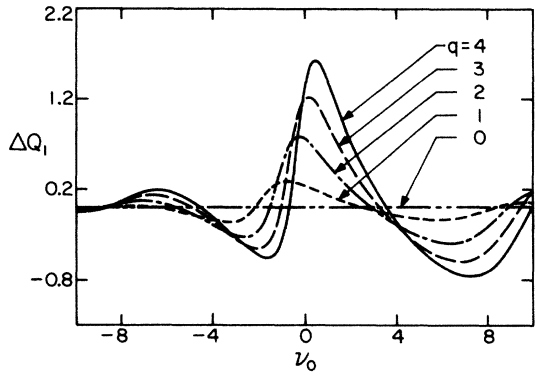

FIG. 13. Changes in Q_1 as a function of ν_0. (Same case as Fig. 11.)

change. This process may also lead to focusing at different values of ν_0.

For most values of ν_0, a combination of localization and focusing occurs. We have plotted the changes in the beam parameters as a function of the detuning in Figs. 11—14 (corresponding to case 1) and 15—18 (case 2). Note that the maxima of Fig. 13 which correspond to localization falls roughly at the zeros of Fig. 14 and vice versa. It is also evident that both effects grow with increasing q. Somewhat different curves were obtained with a finite gradient electron beam in Figs. 15—19. In Fig. 15 we note a substantial difference compared to 1D theory in instances where the electron beam is of smaller diameter than the optical beam. In these cases the maximum gain and phase shift moved away from their "classical" (predicted by one-dimensional theory) positions on the ν_0 axis. This is due to the relatively large changes in the optical-beam profile occurring during a single pass at these values.

CONCLUSION

We have extended the linear one-dimensional FEL theory in several ways. First, we presented an energy theorem that allowed the 3D gain calculation for a given

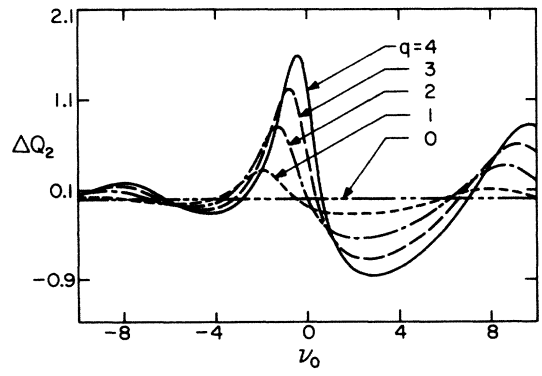

FIG. 14. Changes in Q_2 as a function of ν_0. (Same case as Fig. 11.)

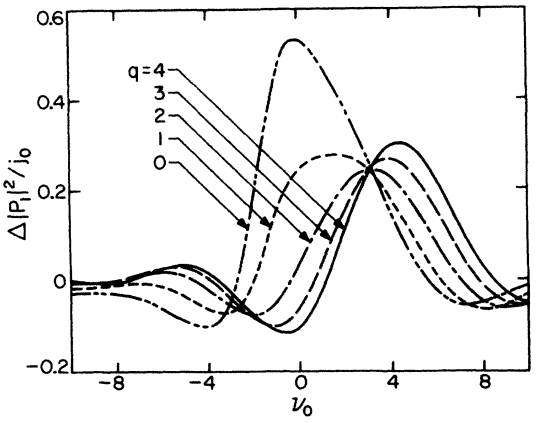

FIG. 15. Changes in P_1 as a function of ν_0. Figures 15—18 are similar to Figs. 11—14 except that the electron beam has a transverse profile ($q_e=5$, $j_0=7$). Note that for $q=0$ (plane wave at $\tau=-\frac{1}{2}$), a relatively large on-axis intensity enhancement occurs at ν_0. This is contrary to the result of 1D theories and is due to the strong focusing induced by the FEL gain medium at this value of the detuning parameter (which is known from 1D theory to produce large phase shifts). As in Figs. 11—14, the zeros and maxima of the focusing and localization alternate.

mode. This expression enabled us to discuss the amplification of a Gaussian beam in a low-gain FEL. We found that optimum gain is achieved at a certain value of the diffraction parameter. The reduction in gain for both larger and smaller values describe the basic mechanism for transverse mode selection by the FEL gain medium. We also investigated finite-width electron-beam profiles and found that the reduction in gain due to nonzero extension of the beam is substantial only for dimensionless areas (q_e^{-1}) of order unity and larger. We considered the possibility of transverse multimode excitation in a confocal resonator and showed that a larger gain may be available provided the system is allowed to oscillate in its own "natural" mode rather than forcing oscillation in a cavity eigenmode.

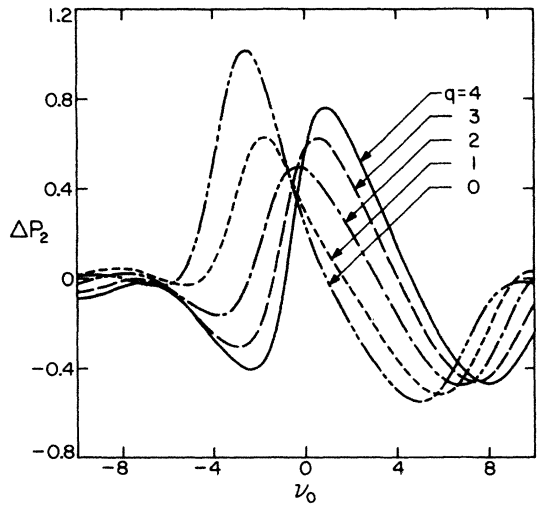

FIG. 16. Changes in P_2 as a function of ν_0. (Same case as Fig. 15.)

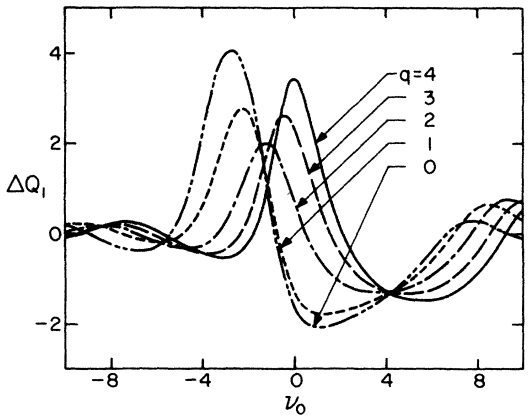

FIG. 17. Changes in Q_1 as a function of ν_0. (Same case as Fig. 15.)

Our gain formula has limited applicability to low-gain cases where the optical mode was assumed to be known and unchanged by the interaction. In order to investigate the high-gain case we have developed a formalism in Sec. IV where the mode develops self-consistently and we have examined the deformation of an input optical beam under the interaction in a single pass. Two mechanisms for confining the beam energy near the axis were described. The gain medium was shown to be capable of both focusing and localizing the optical beam due to its refractive and amplifying components. In both cases there is usually a mixture between the two mechanisms, depending on the value of the detuning parameter. We have distinguished between simple focusing and localization caused by the transverse gradient of the electron-beam profile and that which arises as a result of the electron beam being driven differently across the optical-beam cross section.

The reshaping of the mode resulted in a gain spectrum that may be significantly different than what is expected from a 1D theory or our 3D gain formula with an

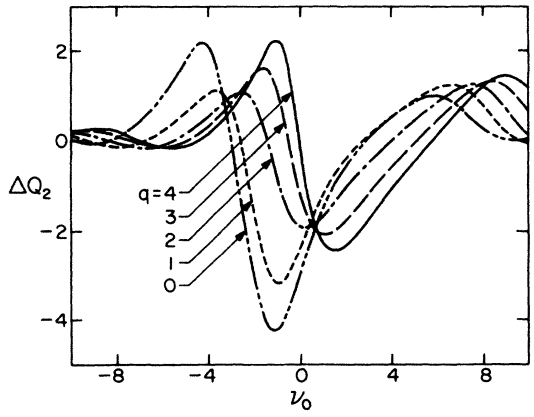

FIG. 18. Changes in Q_2 as a function of ν_0. (Same case as Fig. 15.)

empty-cavity mode. This spectrum can manifest itself in a high-gain amplifier experiment where a scan over input frequencies is made or in an oscillator, in the shift of the lasing mode frequency when compared with the peak spontaneous emission.

Of most current interest is the possibility of constructing a high-gain device operating with nondiffracting (trapped) modes. The existence of such modes is the subject of the subsequent paper[38] in this series.

ACKNOWLEDGMENTS

We would like to acknowledge the contribution of W. B. Colson who initiated some of the ideas developed in this article. This work was supported by the Office of Naval Research (ONR) of the U.S. Department of the Navy under ONR Contract No. N00014-80-C-308.

APPENDIX A: SIMPLIFICATION OF THE GAIN INTEGRAL

In Sec. IV we deal with integrals of the form

$$I=\mathrm{Re}\, i\int d^2r\, j(\mathbf{r})\int_{-1/2}^{1/2}d\tau\int_{-1/2}^{\tau}d\tau'\int_{-1/2}^{\tau'}d\tau''\, e^{-i\nu_0(\tau-\tau'')}f^*(\mathbf{r},\tau)f(\mathbf{r},\tau'')\ .$$

Integrating by parts eliminates the τ' integral

$$I=\mathrm{Re}\, i\int d^2r\, j(\mathbf{r})\int_{-1/2}^{1/2}d\tau\int_{-1/2}^{\tau}d\tau'(\tau-\tau')e^{-i\nu_0(\tau-\tau')}f^*(\mathbf{r},\tau)f(\mathbf{r},\tau')\ ,$$

where we have renamed τ'' as τ'. The last expression can be written more compactly as

$$I=\mathrm{Re}(-1)\int j(\mathbf{r})d^2r\frac{\partial}{\partial\nu_0}\int_{-1/2}^{1/2}d\tau'\, e^{-i\nu_0(\tau-\tau')}f^*(\mathbf{r},\tau)f(\mathbf{r},\tau')\ .$$

Note that $\mathrm{Re}[e^{-i\nu_0(\tau-\tau')}f^*(\mathbf{r},\tau)f(\mathbf{r},\tau')]$ is symmetric under the exchange of τ and τ'. This property may be used to decouple the double integral as follows (omitting the $\mathbf{r}$ dependence for brevity)

$$\mathrm{Re}\int_{-1/2}^{1/2}d\tau\int_{-1/2}^{\tau}d\tau'\, e^{-i\nu_0(\tau-\tau')}f^*(\tau)f(\tau')$$
$$=\tfrac{1}{2}\,\mathrm{Re}\int_{-1/2}^{1/2}d\tau\int_{-1/2}^{\tau}d\tau'\, e^{-i\nu_0(\tau-\tau')}f^*(\tau)f(\tau')+\tfrac{1}{2}\,\mathrm{Re}\int_{-1/2}^{1/2}d\tau\int_{\tau}^{1/2}d\tau'\, e^{-i\nu_0(\tau-\tau')}f^*(\tau)f(\tau')\ ,$$

where in the last integrals we have changed the order of integration.

Thus we get

$$I=-\frac{1}{2}\frac{\partial}{\partial\nu_0}\int j(\mathbf{r})d^2r\left|\int_{-1/2}^{1/2}d\tau\, e^{i\nu_0\tau}f(\mathbf{r},\tau)\right|^2\ .$$

Finally we note that the numerical computation of the integrals

$$J(\nu_0)=\frac{\partial}{\partial\nu_0}\left|\int_{-1/2}^{1/2}d\tau\, e^{i\nu_0\tau}f(\mathbf{r},\tau)\right|^2$$

is most conveniently carried out in the form

$$J(\nu_0)=2\,\mathrm{Re}\int_{-1/2}^{1/2}d\tau\,\tau e^{i\nu_0\tau}f(\mathbf{r},\tau)\times\int_{-1/2}^{1/2}d\tau\, e^{-i\nu_0\tau}f^*(\mathbf{r},\tau)\ .$$

APPENDIX B: CONVERSION OF EQUATIONS (5.4) TO A SET OF ORDINARY DIFFERENTIAL EQUATIONS

We define the variable U and V as

$$U=\int_{-1/2}^{\tau}(\tau-\tau')e^{i\nu_0\tau'}P(\tau')d\tau'\ ,$$
$$V=\int_{-1/2}^{\tau}(\tau-\tau')e^{i\nu_0\tau'}P(\tau')Q(\tau')d\tau'\ ,$$

to get the following set of ordinary differential equations of the second order:

$$P'=iPQ+\tfrac{1}{2}ij_0Ue^{-i\nu_0\tau}\ ,$$
$$Q'=iQ^2+\tfrac{1}{2}ij_0P^{-1}[V-U(Q+q_e)]e^{-i\nu_0\tau}\ ,$$
$$U''=Pe^{i\nu_0\tau},\quad V''=PQe^{i\nu_0\tau}\ .$$

The initial conditions for U and V are obtained from their definitions: $U'(-\frac{1}{2})=U'(-\frac{1}{2})=0$ and $V'(-\frac{1}{2})=V(-\frac{1}{2})=0$.

---

[1]See, for example: (a) *Physics of Quantum Electronics*, edited by S. Jacobs and M. Sargent (Addison-Wesley, Reading, MA, 1982), Vols. 5 and 7–9; (b) IEEE J. Quantum Electron. **QE-17** (1981). (c) *ibid.* **QE-19** (1983). (d) Proc. SPIE **453** (1983).

[2]W. B. Colson, in Ref. 1(a), Vol. 5, p. 157.

[3]N. M. Kroll, *et al.*, in Ref. 1(a), Vol. 7, p. 89; P. Sprangle *et al.*, in Ref. 1(a), Vol. 7, p. 207.

[4]W. B. Colson, in Ref. 1(a), Vol. 9, pp. 457–488; G. Datolli *et al.*, *ibid.*, pp. 515–530.
[5]L. R. Elias *et al.*, Phys. Rev. Lett. **36**, 717 (1976).
[6]D. A. G. Deacon *et al.*, Phys. Rev. Lett. **38**, 892 (1976).
[7]M. Billardon *et al.*, Phys. Rev. Lett. **51**, 1652 (1983).
[8]A. Amir *et al.*, Appl. Phys. Lett. **47**, 1257 (1985); L. Elias *et al.*, Phys. Rev. Lett. **57**, 424 (1986).
[9]D. A. G. Deacon (private communication).
[10]A. Yariv, *Quantum Electronics*, 2nd ed. (Wiley, New York, 1975).
[11]H. Kogelnik and W. Rigrod, Proc. IRE **50**, 230 (1962); A. E. Siegman, *An Introduction to Lasers and Masers* (McGraw-Hill, New York, 1968). For observation of transverse mode mixing in FEL see: D. A. G. Deacon *et al.*, IEEE J. Quantum Electron. **QE-21**, 208 (1985).
[12]Y. R. Shen, Prog. Quantum Electron. **4**, (1975).
[13]J. H. Marburger, Ref. 12, pp. 35–110.
[14]A. K. Ghatak, *Contemporary Optics* (Plenum, New York, 1978), Chap. 10.
[15]M. Born and E. Wolf, *Principles of Optics*, 6th ed. (Pergamon, New York, 1980).
[16]C. Tang and P. Sprangle, in Ref. 1(a), Vol. 9, p. 627.
[17]C. Tang and P. Sprangle, *Proceedings of the International Conference on Lasers, 1982*, edited by R. C. Powel (STS, McLean, Virginia, 1982), p. 177.
[18]W. B. Colson and P. Elleaume, Appl. Phys. B **29**, 101 (1982).
[19]A. Amir and L. Elias, in *Lasers in Fluid Mechanics and Plasmadynamics*, Proceedings of the AIAA 16th Conference, edited by C. P. Wang (American Institute of Aeronautics and Astronautics, New York, 1983).
[20]A. G. Fox and T. Li, Bell Syst. Tech. J. **41**, 453 (1961).
[21]D. Prosnitz, R. A. Haas, S. Doss, and R. J. Galinas, in Ref. 1(a), Vol. 9, p. 531.
[22]S. A. Mani, D. A. Kroff, and J. Blimmel, in Ref. 1(a), Vol. 9, pp. 557–575.
[23]D. C. Quimby and J. Slater, IEEE J. Quantum Electron. **QE-19**, 800 (1983).
[24]J. M. Slater and D. D. Lowenthal, J. Appl. Phys. **52**, 44 (1981).
[25]C. J. Elliot, in Ref. 1(a), Vol. 8, p. 531.
[26]B. J. Coffey, M. Lax, and C. J. Elliot, IEEE J. Quantum Electron. **QE-19**, 297 (1983).
[27]W. B. Colson and J. L. Richardson, Phys. Rev. Lett. **50**, 1050 (1983).
[28]C. J. Elliot, J. Phys. (Paris) Colloq. **44**, C1-255 (1983).
[29]D. A. Deacon and P. Elleaume, Appl. Phys. B **33**, 9 (1984).
[30]A. E. Siegman and E. A. Sziklas, Appl. Opt. **13**, 2775 (1974).
[31]E. A. Sziklas and A. E. Siegman, Appl. Opt. **14**, 1874 (1975).
[32]B. N. Perry, P. Rabinowitz and M. Newstein, Phys. Rev. Lett. **49**, 1921 (1982).
[33]N. S. Ginzburg, N. F. Kovalev, and N. Yu Rusov, Opt. Commun. **46**, 300 (1983).
[34]E. T. Scharlemann *et al.*, Phys. Rev. Lett. **54**, 1925 (1985); G. T. Moore, Opt. Commun. **52**, 46 (1984).
[35]J. M. J. Madey, Nuovo Cimento B **50**, 64 (1979).
[36]A. Amir *et al.*, Phys. Rev. A **32**, 2864 (1985).
[37]A. Amir and Y. Greenzweig, Proceedings of the Seventh International Free-Electron Laser Conference, Tahoe City, California, 1985 [Nucl. Instrum. Methods Phys. **A250**, 404 (1986)].
[38]A. Amir and Y. Greenzweig (unpublished).
[39]L. Casperson and A. Yariv, Appl. Phys. Lett. **12**, 355 (1968).